Separation Science and Technology
Publication details, including instructions for authors and subscription information:
http://www.informaworld.com/smpp/title~content=t713708471

Influence of Hydrolysis Mechanisms on Molybdate Sorption Isotherms Using Chitosan

Eric Guibal[a]; Céline Milot[a]; Jean Roussy[a]
[a] LABORATOIRE GÉNIE DE LENVIRONNEMENT INDUSTRIEL, ALÈS CEDEX, FRANCE

Online publication date: 16 May 2000

To cite this Article Guibal, Eric , Milot, Céline and Roussy, Jean(2000) 'Influence of Hydrolysis Mechanisms on Molybdate Sorption Isotherms Using Chitosan', Separation Science and Technology, 35: 7, 1021 — 1038
To link to this Article: DOI: 10.1081/SS-100100208
URL: http://dx.doi.org/10.1081/SS-100100208

SEPARATION SCIENCE AND TECHNOLOGY, **35**(7), pp. 1021–1038, 2000

Influence of Hydrolysis Mechanisms on Molybdate Sorption Isotherms Using Chitosan

ERIC GUIBAL,* CÉLINE MILOT, and JEAN ROUSSY
ECOLE DES MINES D'ALÈS
LABORATOIRE GÉNIE DE L'ENVIRONNEMENT INDUSTRIEL
6, AVENUE DE CLAVIÈRES, F-30319 ALÈS CEDEX, FRANCE

ABSTRACT

Molybdate sorption using chitosan sorbents has proved to be strictly controlled by the pH of the solution. Sorption isotherms exhibit a sigmoid trend, which has been correlated to the appearance of polynuclear hydrolyzed species, the most favorable species for sorption on chitosan. Sorption capacity exceeds 7 $mmol \cdot g^{-1}$, which corresponds to a molar ratio between Mo and the amine group significantly higher than 1. The formation of complexes in a pendant fashion and/or the ion-exchange mechanism of polynuclear metal ions are suspected to occur between polynuclear molybdate species and protonated amine groups, though several amine groups can interact with the same polynuclear molybdate group.

Key Words. Chitosan; Molybdate; Hydrolysis; Sorption; Isotherms; pH

INTRODUCTION

For the last thirty years many studies have focused on the biosorption of metal ions on various sorbents: bacteriae, fungi, and algae, or waste biomaterials, have been commonly studied for the recovery of metal cations (1–3). Several mechanisms can be involved in the uptake process, such as active transport of metals through the cellular membrane or passive sorption on membrane constitutents (4). Passive phenomena usually involve ion exchange (5), adsorption, complexation, or in-situ precipitation (6). The potential binding sites of biosorbents are amino, carboxyl, phosphate, hydroxyl, and sulfate

* To whom correspondence should be addressed.

groups. The interpretation of sorption mechanisms is rendered complex by the diversity of functional groups constituting cell walls. Several biopolymers which can be encountered in these cell walls have been studied and used as an alternative to biosorbents; e.g., alginate (7, 8) and chitosan (9). Using simple biopolymers makes it easier to identify the sorption mechanisms (10) and interpret the effect of the experimental parameters (pH, metal concentration) on sorption efficiency.

The influence of the pH on sorption performance is mainly attributed to electrostatic attraction or repulsion between the metal ions and the sorption sites. While many studies have dealt with metal cation sorption, the literature is less abundant on metal anion removal using biosorbents. These studies have been mainly devoted to simple metals, in the sense these metals usually occur in solution as mononuclear species with few hydrolyzed forms. The differences in the behavior of sorbents with respect to pH and metal concentration are sometimes interpreted as the co-existence of several binding sites (11). However, it seems that the influence of hydrolysis mechanisms has been underestimated in evaluation of the pH effect as stated for metal ion sorption on mineral sorbents. It has been shown that with mineral surfaces, metal ion sorption (efficiency and capacity) usually increases drastically in the pH region in which metal hydrolysis occurs.

Baes and Mesmer compiled the hydrolysis constants of metal cations (Table 1) and showed the distribution of metal ions to be a function of pH and total metal concentration (12). This work highlights the importance of polynuclear hydrolyzed species. In the present work molybdate sorption is investigated with respect to the effect of pH on sorption isotherms by using a sorbent

TABLE 1
Equilibria of MoO_4^{2-} at 25°C: Formation Constants from Baes and Mesmer (12)

$$xMoO_4^{2-} + yH^+ \rightleftarrows Mo_xO_z(OH)_{8x-y-2z}^{(2x-y)-} + (y - 4x + z)H_2O$$

x	y	pK	Mo species
1	1	3.89	$HMoO_4^-$
1	2	7.5	H_2MoO_4
7	8	57.74	$Mo_7O_{24}^{6-}$
7	9	62.14	$Mo_7O_{23}(OH)^{5-}$
7	10	65.68	$Mo_7O_{22}(OH)_2^{4-}$
7	11	68.21	$Mo_7O_{21}(OH)_3^{3-}$
19	34	196.30	$Mo_{19}O_{59}^{4-}$ [a]

[a] This species has been neglected in the calculation of speciation diagrams in the pH range selected in this study. Calculations were made using HYDRAQL software (28).

MARCEL DEKKER, INC.
270 Madison Avenue, New York, New York 10016

derived from chitosan. The variation in sorption capacities, as well as the variation in the shape of the sorption isotherms with pH, is also discussed in relation to metal speciation in solution. Chitosan (poly[β-(1→4)-2-amino-2-deoxy-D-glucopyranose]) is produced by the deacetylation of chitin (poly[β-(1→4)-2-acetamido-2-deoxy-D-glucopyranose]), a widely dispersed natural biopolymer encountered in arthropods and crustacea shells (13). Chitosan is partially soluble in mineral acids, such as nitric and hydrochloric acids, but almost insoluble in sulfuric acid (at a molar concentration). The chemical resistance to dissolution can be easily increased by a crosslinking step using a Schiff's base reaction with glutaraldehyde. Molybdate is widely used in the fabrication of catalysts for petrochemical applications, and the impregnation of a catalytic carrier with molybdate involves the production of highly concentrated solutions which must be treated before being safely rejected to the environment. Molybdate is also present in many mining effluents from copper minerals, mixed with arsenic, and the recovery/decontamination of acid mine drainage is of great concern. Chitosan-based sorbents have shown a very high affinity for molybdate in both batch and continuous systems (14, 15). Preliminary work has also shown that the optimum sorption for molybdate on chitosan occurs in acid medium and depends on several characteristics of the biopolymer: degree of deacetylation, crystallinity, and to a lesser extent molecular weight (16). Molybdate interactions with chitosan have also been studied by Draget et al. (17). They showed that the reaction of chitosan with molybdate at a high concentration (20 mM—almost 2 $g \cdot L^{-1}$) and at a moderately acidic pH (i.e., pH 5) allows gelation of the system and crosslinking of chitosan. The sorbent used in the present study is a glutaraldehyde crosslinked chitosan. The recycling of the sorbent after exhaustion can be performed with alkaline solutions, which allows the sorbent to be reused for several sorption/desorption cycles: the process can be applied for both metal recovery and recycling and for environmental purposes.

MATERIAL AND METHODS

Chitosan Samples

Chitosan was supplied by ABER-Technologie (France) as a flaked material, with an acetylation fraction FA ca. 0.13 (defined by IR spectrometry) (18). The mean molecular weight was measured as 125,000 [using a size exclusion chromatography (SEC) method with a differential refractometer and a multiangle laser light-scattering photometer for detection] (19).

Chemical crosslinking of chitosan chains with the bifunctional reagent glutaraldehyde occurs by a Schiff's reaction of the aldehyde groups on glutaraldehyde with the amine groups on the chitosan biopolymer chain (13). The crosslinking bath contained a 2.5 wt% glutaraldehyde solution. The ratio of

glutaraldehyde to chitosan flakes was approximately 2 $cm^3 \cdot g^{-1}$ of flakes. Crosslinking occurred for 16 hours. The crosslinked chitosan beads were extensively rinsed with demineralized water. Similar procedures were applied to manufacture crosslinked chitosan flakes in three particle sizes: G1 $<$ 125 μm, G2 $<$ 250 μm, G3 $<$ 500 μm. Dissolution testing in sulfuric acid solutions (pH ca. 3) showed that chitosan does not significantly dissolved after the crosslinking step; the chitosan concentration in the solution was measured using the acid red titration method (20). These findings demonstrate that the crosslinking is stable in our experimental conditions.

The specific surface area was measured by the BET method and gave a value of approximately 1 $m^2 \cdot g^{-1}$ (21). Due to the low porosity of the chitosan biopolymer, this determination is not as accurate as with the usual sorbents; however, it does give an approximation of the contact surface.

Experimental Procedure: Metal Ion Adsorption

Ammonium molybdate salts were used. Sorption isotherms were determined by contact of 200 mL of molybdate (of varying initial metal ion concentrations: ca. 50, 100, and 200 $mg \cdot L^{-1}$, corresponding to molar concentrations of 0.52, 1.04, and 2.08 $mmol \cdot L^{-1}$) with known weights of crosslinked chitosan flakes (dry sorbent masses varying between 20 and 200 mg). All experiments were performed at room temperature with a constant pH control achieved by adding microvolumes of molar sodium hydroxide or sulfuric acid solutions. Samples were collected and separated (filtration through a 1.2-μm pore glass fiber membrane) after 72 hours of agitation using an adjustable reciprocating shaker (150 rpm). The metal ion content was determined by ICP spectrometry. The metal ion content in the solid, q ($mg \cdot g^{-1}$ or alternatively $mmol \cdot g^{-1}$), was determined by a mass balance (between solid and liquid phases). All metal concentrations in both solid and liquid media are expressed in this paper as total metal (mg) in order to be independent from the form of the metal ion (free molybdate or hydrolyzed species, etc.,) while the sorbate is called “molybdate ion” as a general term.

Potentiometric Titrations

A known mass (usually 20 mg) of chitosan sample was added to a closed flask containing 100 mL of solution: demineralized water of sodium sulfate (0.05 or 0.1 M). The sorbent’s particles remained in contact with the solution for 72 hours on a reciprocal shaker. The titrations were carried out by using sulfuric acid solutions (concentrations: 1 M, 0.1 M, 0.01 M). An equilibrium time of 3 hours was observed between each titration step; agitation of the solution was maintained and the flask closed to avoid carbon dioxide dissolution. Titration of the sorbent made it possible to determine the surface charge

MARCEL DEKKER, INC.
270 Madison Avenue, New York, New York 10016

($C \cdot m^{-2}$) as suggested by Chen and Yiacoumi (8):

$$\sigma_0 = \frac{(C_a - C_b + [OH^-] - [H_3O^+])F}{Sa} \quad (1)$$

where C_a and C_b are the concentrations of acid or base needed to reach a point on the titration curve in $mol \cdot L^{-1}$; $[H_3O^+]$ and $[OH^-]$ are the concentrations of H_3O^+ and OH^- (in $mol \cdot L^{-1}$) deduced from the pH and adjusted by the Davis equation (22, Eq. 2); F is the Faraday constant (96,490 $C \cdot mol^{-1}$); S is the specific surface area (about 1000 $m^2 \cdot kg^{-1}$, measured by the BET method); and a is the sorbent concentration in the solution ($kg \cdot L^{-1}$).

$$\log \gamma_i = -0.5109 \left(\frac{\sqrt{I}}{1 + \sqrt{I}} - 0.3\, I \right), \qquad I = 0.5 \sum_i C_i z_i^2 \quad (2)$$

where γ_i is the activity coefficient of component i (concentration C_i, ionic charge Z_i), and I is the ionic strength ($mol \cdot L^{-1}$).

RESULTS AND DISCUSSION

Potentiometric Titration

The surface charge varies drastically as a function of the pH of the solution as shown in Fig. 1. Decreasing the pH involves a strong increase in the positive charge of the sorbent. This expected result is consistent with the pK_a of chitosan. Several examples have been reported regarding the value of the pK_a of chitosan (ranging from 6.2 to 6.8) (13). However, these first results have not taken into consideration the effect of chain charge density. Domard (23), us-

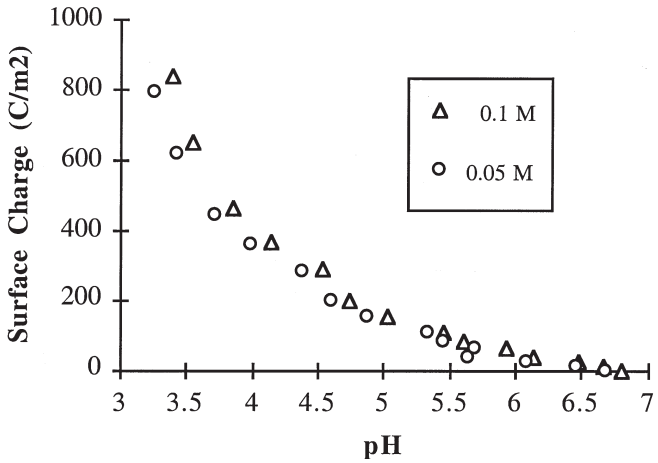

FIG. 1 Effect of pH on surface charge for crosslinked chitosan flakes (ionic strength fixed with sodium sulfate).

MARCEL DEKKER, INC.
270 Madison Avenue, New York, New York 10016

ing potentiometric and circular dichroism measurements, has shown that the variation of the pK_a obeys the Katchalski–Spitinik equation and can be related to the difference in electrostatic potential between the surface of the polyion and the reference $\Delta\Psi(\alpha)$.

$$pK_a = pH + \log\left(\frac{1-\alpha}{\alpha}\right) = pK_0 - \frac{\varepsilon\Delta\Psi(\alpha)}{kT} \quad (3)$$

where α is the degree of neutralization of the polymer, pK_0 is the intrinsic dissociation constant of the ionizable groups, ε is the charge of the electron, and kT is the Boltzmann term. The intrinsic dissociation constant pK_0 is independent of the degree of *N*-acetylation (conversely to pK_a) and equals 6.5 (extrapolation of the pK_a value to $\alpha = 1$). From the results of Domard (23), it appears that the pK_a of chitosan strongly varies with the degree of dissociation for chitosan of low acetylation fraction (lower than FA = 0.15), while for higher FA the pK_a hardly varies with the degree of dissociation around 6.4–6.5.

Figure 1 shows that the surface charge becomes positive for pH lower than 6.5, a pH value corresponding to the pK_a of the raw material. It is surprising to see that the surface charge has already dropped to 0 at a pH equal to the pK_a value where 50% of the amino groups are still positively charged. This result can be due to a change in the actual pK_a of the modified sorbent through a reduction of the number of free amino groups. However, Domard (23) has shown that the pK_a is less influenced by the neutralization of amino groups for high FA than for low-acetylated chitosan: with high FA the pK_a is almost independent of the neutralization yield. The grafting of glutaraldehyde moities on the chitosan backbone is expected to lead to the formation of a polymer similar to a high FA chitosan. On the other hand, Roberts observed that in the 6–7 pH range the actual pH values depend on the conditions used in the titration; the values obtained in a continuous titration procedure are considerably higher than those obtained by allowing the system to stand, with stirring, for 36 hours before measuring the pH (13). Differences greater than 0.5 of a pH unit were obtained at some degrees of neutralization. Domard suggested that the delay between partial neutralization and pH measurement allowed partial precipitation of neutralized chain segments to occur, effectively removing amino groups from solution and thereby increasing the extent of dissociation of the amino groups which remain in solution when titration is performed by alkaline addition to an acid solution of chitosan. In this work the pH equilibration lasted at least 3 hours during titration; the initial pH, just after acid addition, is noted and compared to the equilibrium pH. Below pH 3.5, as expected, the difference between these pH values is not significant and the sorbent is fully protonated: this limit value is 3 pH units lower than the pK_a value, and the protonation yield reaches 99.9%. For higher pH it is not certain that equilibrium is actually reached, and thus the low positive charge of the

MARCEL DEKKER, INC.
270 Madison Avenue, New York, New York 10016

sorbent observed at a pH approximate to the pK_a of chitosan may be indicative of a pH higher than 5–5.5. The fraction of protonation of the amino groups in the sorbent depends on the pH. However, as indicated above, and with the restrictions evoked regarding moderate acidic solutions, in very acidic solution the sorbent may be considered to be fully protonated, for pH values lower than 5.5, more than 90% of the amino groups are protonated, and up to 6.5 the fraction progressively decreases. The surface charge, σ_0, as shown in Fig. 1, is consequently significant until pH 3.5 and $\sigma_0 = 600\ C \cdot m^{-2}$. The ionic strength hardly changes the surface charge, the largest variation being obtained at the lowest pHs.

Sorption Isotherms

Figure 2 shows the sorption isotherms obtained at several controlled pHs. These curves clearly demonstrate that both the maximum uptake capacity and shape of the curves depend on the pH. For acid media, around pH 3, a favorable sorption isotherm with a convex form is obtained. For pH values ranging between 5 and 8, the sorption isotherms are characterized by a concave form. The curve tends to zero for the lowest concentrations and can be classified as unfavorable sorption isotherms. Beyond a limit concentration, the uptake capacity increases strongly. This limit pH is not uniform and depends on the overall concentrations; it can be related to hydrolysis mechanisms, as it will be discussed below.

The optimum pH is lower than 4. This is consistent with previous results on molybdenum extraction from solutions using liquid–liquid extraction (24, 25). However, the behavior of the extraction system depends on the extrac-

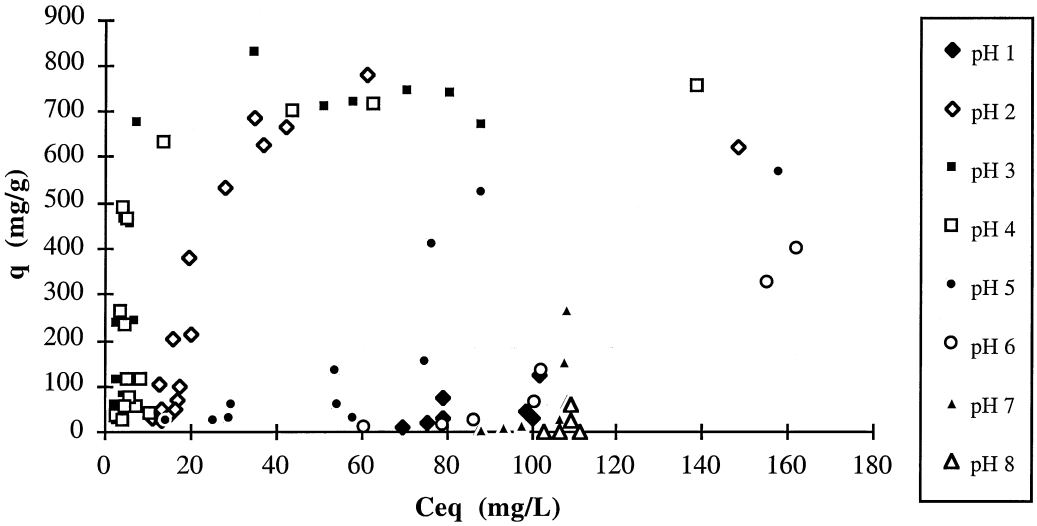

FIG. 2 Effect of pH on molybdate sorption on crosslinked chitosan beads.

tant while the extraction efficiency is independent of pH below 3–4 in most parts of our studies, for some of these systems the extraction efficiency decreases significantly for the most acidic solutions (below pH 1). The influence of the pH is related to the formation of a cationic species, MoO_2^{2+}, favorable for extraction by cation exchange with suitable extractants; for example, Cyanex 272, PIA-8, and PC-88A (25). However, this species can only be obtained in concentrated solutions, such as those obtained in the recovery of molybdenum from spent catalysts. Anionic species are formed in dilute solutions (12, 26). The speciation of molybdate has been extensively studied in acidic solutions by Tytko et al. They showed that the chemistry of molybdate is complicated by the presence of several different anionic species whose predominance is controlled by both the pH and total molybdenum concentration (27). Pope stated that the first stable polyanions formed (pH ca. 5) in aqueous solutions are the heptametalates, the so-called paramolybdates, and their subsequent hydrolysis compounds (28). At high molybdate concentration and intermediary pH the predominant species is $Mo_7O_{24}^{6-}$. However, several other species coexist with comparable relative concentrations at lower pH and lower total concentration.

Figure 3 shows the distribution of molybdate species as a function of pH and metal concentration. Calculations were performed with the HYDRAQL software (29) using the constants from Baes and Mesmer (12) reported in Table 1. The figure clearly demonstrates that the distribution of metal ions varies with both parameters. Tytko et al. (27) cited the formation of other complementary polymolybdate species but in a higher concentration range than that investigated in this study. In acidic solution with moderate concentrations the predominant species are the polynuclear forms: $Mo_7O_{24}^{6-}$, $Mo_7O_{23}(OH)^{5-}$, and $Mo_7O_{22}(OH)_2^{4-}$. They are thus characterized by a strong anionic charge convenient for electrostatic attraction onto the chitosan sorbent, whose surface charge in acidic solutions is strongly positive (Fig. 1). This conclusion is consistent with results cited by Draget et al. for the molybdate crosslinking of chitosan (17). The gels were obtained by dispersing solid MoO_3 in a buffered chitosan solution: the crosslinking results from the reaction of protonated amino groups with heavily negatively charged molybdate polyoxyanions. Juang and Ju used these electrostatic mechanisms to increase sorption efficiency/selectivity in copper recovery in acidic solutions by using a preliminary EDTA-chelating step (30). The chelation of copper with EDTA allows the complex to be negatively charged and suitable for sorption on positive chitosan surfaces. Yoshida et al. interpreted similar electrostatic effects of dye sorption on chitosan sorbents (31).

It has been suggested that pH control with sulfuric acid involves protonation of the amine sites and the presence of HSO_4^- and/or SO_4^{2-} in the neighborhood of the binding sites. Inoue et al. propose this mechanism for palla-

MARCEL DEKKER, INC.
270 Madison Avenue, New York, New York 10016

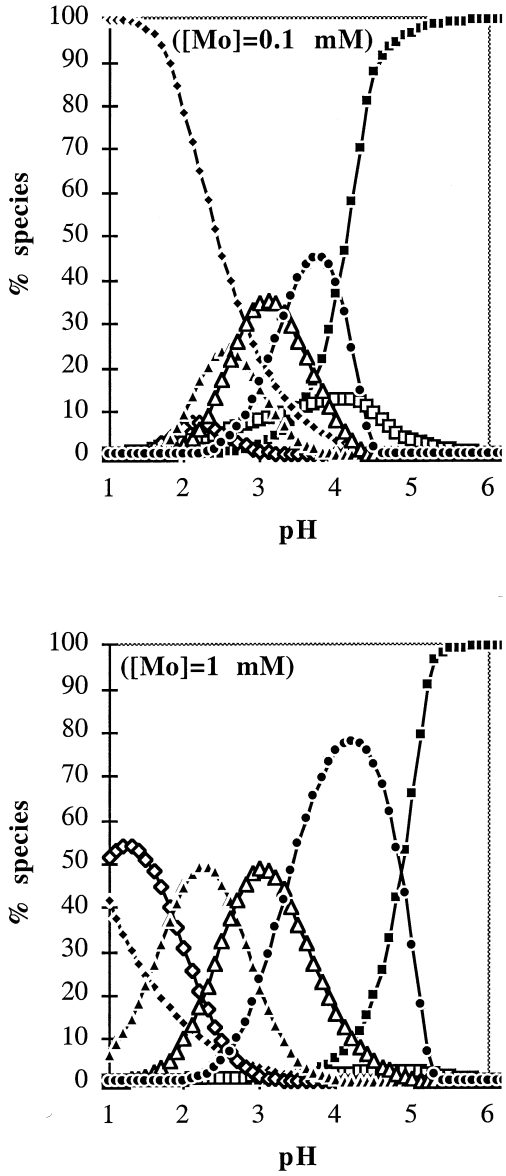

FIG. 3 Influence of pH and total molybdate concentration on speciation (■: MoO_4^{2-}, □: $HMoO_4^-$, ◆: H_2MoO_4, ◊: $Mo_7O_{21}(OH)_3^{3-}$, ▲: $Mo_7O_{22}(OH)_2^{4-}$, △: $Mo_7O_{23}(OH)^{5-}$, ●: $Mo_7O_{24}^{6-}$).

dium and platinum anion recovery on substituted chitosan sorbents (32). The counterion is mainly HSO_4^- for pH lower than 2, while sulfate predominates at higher pH, and molybdate sorption occurs by anion exchange on positively charged nitrogen sites.

For the optimum pH (ca. 2–4 pH range), the maximum uptake capacity reaches almost 8 $mmol \cdot g^{-1}$. Taking into account the FA of the chitosan sam-

ple (0.13), the molecular weight of the average monomer unit is obtained using the following formula:

$$M = 161(1 - \mathrm{FA}) + 203\mathrm{FA} \quad (4)$$

where 161 represents the molecular weight of the glucosamine residue and 203 represents that of the acetylglucosamine residue in the polymer.

The amine content in 1 g of polymer is thus 6 mmol, and consequently the molybdate/amine ratio reaches almost 1.3 mmol Mo/mmol NH_2, for the optimum pH. A molar ratio exceeding 1 clearly demonstrates that polynuclear species are involved in molybdate accumulation.

Distribution Coefficient

The distribution coefficient, calculated as the ratio of the solute content in the solid phase to its content in the liquid phase, has been widely used to describe the equilibrium transfer of metal ions to a chitosan-like sorbent (32). Figure 4 represents the evolution of the distribution coefficient with the pH. For each individual pH value the related distribution coefficient was determined as the mean of values obtained from three different experimental sets (corresponding to three sorbent dosages).

Inoue et al. showed that for most metal ions the distribution ratio continuously increases with increasing pH when using modified chitosan sorbents. They showed that the plots lie on a straight line whose slope equals the valence of the adsorbed metal ions (32). Some of the metals investigated do not obey this trend, and the difference is attributed to the possible oxidation of the metal

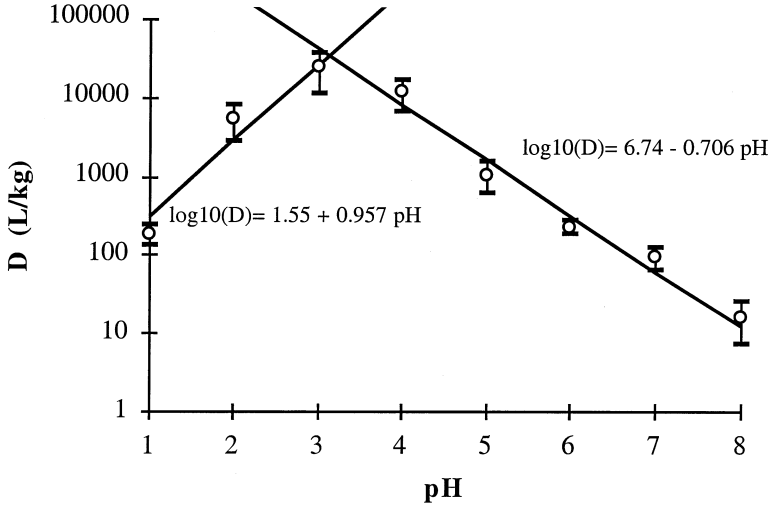

FIG. 4 pH effect on the distribution coefficient for molybdate uptake on crosslinked chitosan beads (○: experimental data; I: standard deviation range, obtained from experimental sets with different sorbent concentrations; solid lines: linearization of distribution coefficient with pH).

[Co(II) to Co(III)] or to the ionic charge of the metal [VO^{2+} for V(IV)]. They related these behaviors to the observations made on the solvent extraction of cationic metal ions with acidic and/or chelating extractants, and explained that the metal ions are adsorbed through a cation-exchange mechanism. They observed a specific behavior for molybdate sorption, and attributed the difference to the formation of the unadsorptive anionic species $HMoO_4^-$ and MoO_4^{2-}. However, the present results cannot be directly compared to the study of Inoue because of the differences in experimental procedures especially metal concentrations (significantly lower in the present work) and the pH control imposed in this study [while Inoue et al. (32) only used the equilibrium pH].

We observe that in the first part of the curve, from pH 1 to pH 3, the slope of the curve tends to 0.96. In the second part of the curve the slope tends to -0.71, which can be compared to the relative charge of ionic molybdate species: $MoO_4^{2-}/-2$; $HMoO_4^-/-1$; $Mo_7O_{21}(OH)_3^{3-}/-3/7$, $Mo_7O_{22}(OH)_2^{4-}/-4/7$, $Mo_7O_{23}(OH)^{5-}/-5/7 = -0.71$; $Mo_7O_{24}^{6-}/-6/7$. The most favorable molybdate species thus seems to be the $Mo_7O_{23}(OH)^{5-}$ form.

The stoichiometry between amine sites and molybdate at maximum uptake is not consistent with such ratios, and this indicates that molybdate sorption does not lead to a neutralization of the overall charge of the sorbent. The existence of pendant complexes has been cited in the case of copper sorption on chitosan (23), while several other configurations/mechanisms were suggested for other metal ions such as ion pair formation for palladium and platinum (32) and a template effect for copper on tailor-made chitosan (33).

Contribution of Hydrolysis Mechanisms in Molybdate Uptake

Figure 2 showed that sorption isotherms are strongly influenced by the pH of the solution in both maximum sorption capacity and affinity coefficient (coefficient *b* of the Langmuir equation, also related to the initial slope of the sorption isotherm curve). The concentration at which the sorption increases significantly is also a function of the pH. Figure 3 showed that the distribution of molybdate between free and hydrolyzed polynuclear species changes with both pH and metal anion concentration. Figures 5–9 present the sorption isotherms as well as the percentage of mono- versus polynuclear species for pH 1 to 5, respectively. These figures clearly demonstrate that a relationship exists between the concentration at which the sorption capacity increases significantly and the concentration at which polynuclear species begin to appear in the solution. The data points are rather fluctuant and irregular, and the most favorable molybdate species for sorption may change with the pH of the solution. The comparison of individual polyoxyanion concentrations with the sorption isotherm shapes did not give good correlation, and it was prefered to

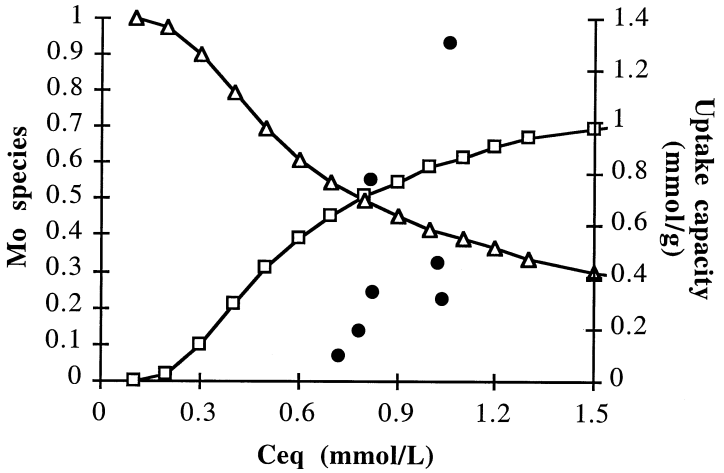

FIG. 5 Molybdate sorption at pH 1 (experimental data: ●) and distribution of molybdate between mono- (△) and polynuclear (□) forms.

correlate the beginning of the sorption curve with the sum of the concentrations of polynuclear hydrolyzed molybdate species.

Since mononuclear molybdate ions exist alone in the solution, the sorbent is not effective at removing metal anions, while for higher residual concentrations in this pH range, the appearance of polynuclear hydrolyzed species involves strong adsorption. Polynuclear hydrolyzed species are characterized by a lower relative ionic charge for molybdate species, as stated below. Their predominance in the best pH–concentration areas indicates that a low relative ionic charge for molybdate anions is required to reach a high sorption level.

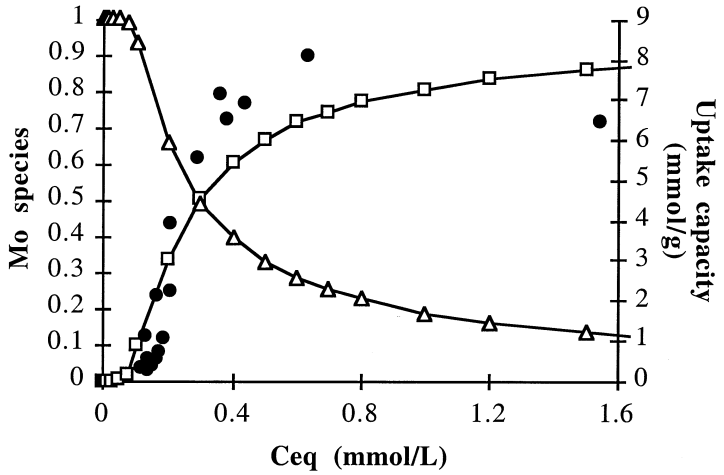

FIG. 6 Molybdate sorption at pH 2 (experimental data: ●) and distribution of molybdate between mono- (△) and polynuclear (□) forms.

MARCEL DEKKER, INC.
270 Madison Avenue, New York, New York 10016

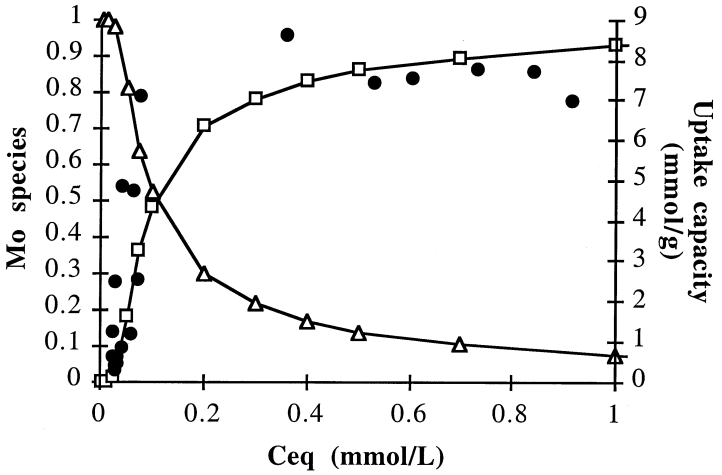

FIG. 7 Molybdate sorption at pH 3 (experimental data: ●) and distribution of molybdate between mono- (△) and polynuclear (□) forms.

The correlation between the "limit" concentrations for sorption capacities and the appearance of polynuclear forms is obvious for pH ranging between 2 and 5. At pH 1 a slight shift appears, though the same global trend is followed. This discrepancy may be explained by either the competitive effect of counterions added to the solution during pH control or by a change in the sorbed species. Indeed, Figure 4 shows that the distribution coefficient can be linearized in two sections with different slopes. Below pH 2 and 2.5, the slope of the curve tends to +1.

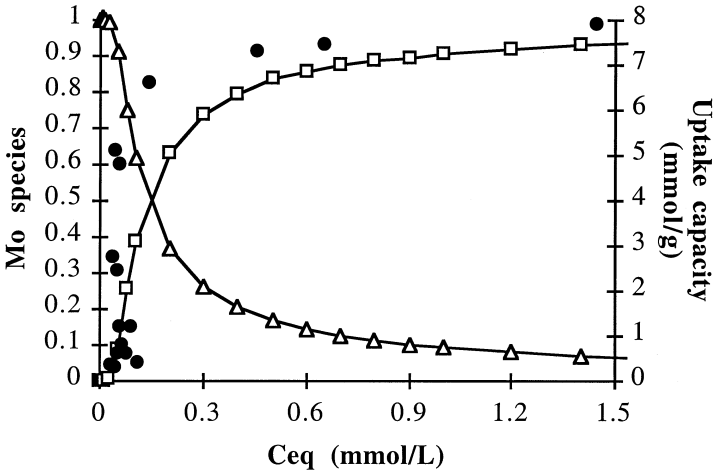

FIG. 8 Molybdate sorption at pH 4 (experimental data: ●) and distribution of molybdate between mono- (△) and polynuclear (□) forms.

MARCEL DEKKER, INC.
270 Madison Avenue, New York, New York 10016

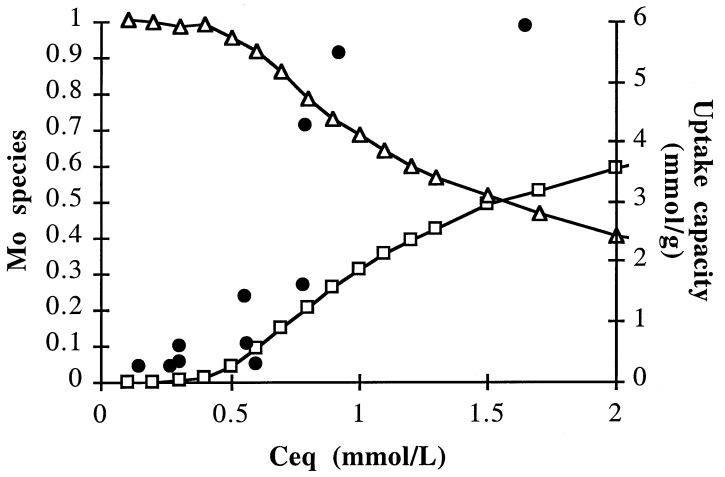

FIG. 9 Molybdate sorption at pH 5 (experimental data: ●) and distribution of molybdate between mono- (△) and polynuclear (□) forms.

Molybdate maximum sorption capacities exceed 7–8 mmol·g^{-1}, and exceed the equimolarity between Mo and N proportions, especially taking into account the reduction in the relative free nitrogen content after glutaraldehyde crosslinking as a complementary confirmation of the sorption of polynuclear species.

Modeling of Sorption Isotherms

In a first attempt to model sorption isotherms that take into account the predominant effect of polynuclear species, sorption capacities were correlated to polynuclear molybdate species concentration using the Langmuir equation. The Langmuir sorption isotherm is

$$q = \frac{q_m b C^*}{1 + bC^*} \tag{5}$$

where C^* is the concentration of polynuclear species (mmol Mo·L^{-1}), q_m is the maximum sorption capacity at monolayer coverage (mmol·g^{-1}), and b is the affinity coefficient of the sorbent for the sorbate (L·mg^{-1}).

Figure 10 shows the polynuclear molybdate species' concentrations as a function of both pH and total molybdenum concentration. The lines represent the linearization of calculated data. The corresponding equations have been used to determine the polynuclear molybdate concentration at equilibrium for experimental data obtained in sorption isotherms. These corrected values of polynuclear molybdate concentrations are taken into account for the modeling of sorption isotherms using the Langmuir model equation. When polynuclear molybdate species exist in solution, the corrected value is used, while for low total concentrations involving only mononuclear species the residual concentration in solution (to be used in the Langmuir model) is made equal to 0 ac-

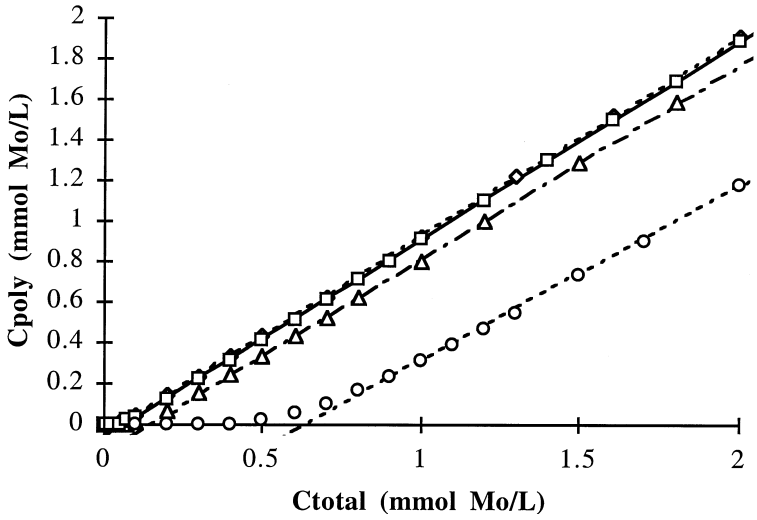

FIG. 10 Molybdate polynuclear species' concentration as a function of total molybdate concentration and pH (experimental points and linearized curves) [(△) pH 2, (◊) pH 3, (□) pH 4, (○) pH 5].

cording to the following equations (6):

$$C^* = C_{\text{polynuclear species}} = \gamma C + \beta, \qquad \text{for } C \geq C_{\text{lim}} = -\beta/\gamma$$
$$C^* = 0, \qquad \text{for } C \leq C_{\text{lim}} = -\beta/\gamma \tag{6}$$

where C_{lim} = concentration for appearance of polynuclear species.

Figure 11 shows a superimposition of experimental points and curves obtained with the Langmuir equation using corrected concentrations for calcula-

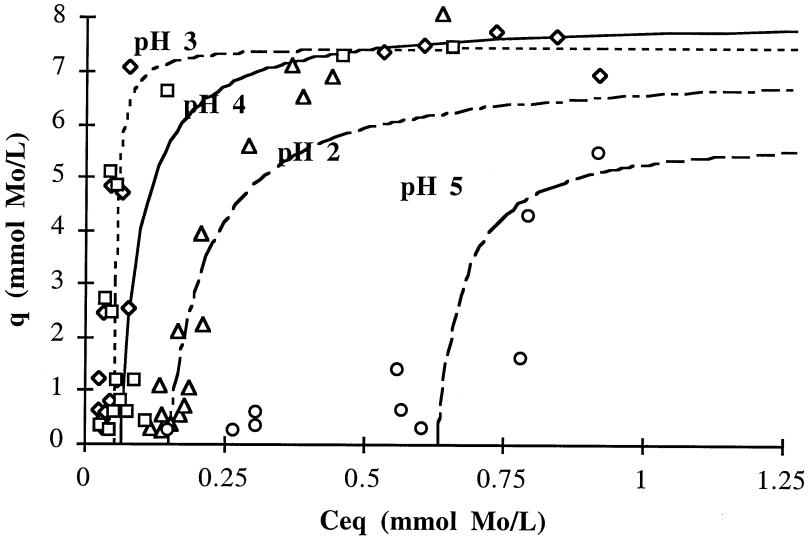

FIG. 11 Experimental data modeling using Langmuir equation for corrected concentrations (polynuclear species' concentrations) [(△) pH 2, (◊) pH 3, (□) pH 4, (○) pH 5].

MARCEL DEKKER, INC.
270 Madison Avenue, New York, New York 10016

tion [the corrected values were converted to the actual total molybdate concentration by using the reciprocal form of Eq. (6) for drawing purposes].

Although the curves do not perfectly fit the experimental points, similar trends are followed, which tend to confirm that the concentration of polynuclear species is the key parameter for molybdate ion sorption on chitosan.

CONCLUSION

Chitosan is effective for removing molybdate with high sorption capacities, exceeding 7 mmol $Mo \cdot g^{-1}$. However, sorption performances are significantly affected by pH, as usually observed for metal ion sorption, but also by the dual effect of pH and metal concentration. The occurrence of hydrolysis mechanisms lead to the formation of polynuclear species whose ionic charge and ionic size are significantly affected by experimental conditions.

The formation of pendant chelates and complexes and/or the ion-exchange interactions of several molybdate moieties (on the same molecule) with several sorption groups (on the biopolymer) may explain why the stoichiometry between free or substituted amine sites and molybdenum exceeds 1. Nekovár and Schrötterová discussed molybdenum(VI) removal using solvent extraction in relation to molybdenum speciation (34). They underlined the influence of polynuclear hydrolyzed species on extraction efficiency, and they discussed the molybdenum to amine stoichiometry in the organic phase in relation to the presence of polymolybdate species.

Optimum sorption occurs in acidic media for which amine sites are strongly protonated: chitosan is one of the most cationic biopolymers. Sorption curves are characterized by a sigmoidal form: an initial part of the curve exhibits very low sorption capacity (corresponding to unfavorable sorption), which is followed by a sharp increase in sorption capacities. The extent of the unfavorable section depends on the pH and is correlated to the concentration at which polynuclear species significantly appear in the solution.

This hypothesis has been confirmed with modeling of sorption curves with the Langmuir equation, taking into account only the sum of the concentrations of polynuclear molybdate species.

These results explain some of the results observed in the sorption of molybdate using chitosan beads crosslinked with glutaraldehyde (14). In a statistical and comparative study of sorption isotherms, obtained with varying initial metal concentrations, it appears difficult to refute the hypothesis that the initial adsorbate concentration influences the sorption capacities. Increasing the metal concentration involves a change in the distribution of metal ion species, and consequently the affinity of the sorbent for metal species.

These results are also consistent with the conclusions of a previous study of the interaction mechanisms between molybdate and chitosan (35). FTIR,

NMR, and surface reflectance techniques have been used for the characterization of molecular interactions, showing that sorbed species depend on the concentration of molybdate in the solution. However, a reduction of molybdenum has been observed on chitosan sorbents, especially when the sorbent is crosslinked with glutaraldehyde. Thus, many chemical and physical interactions occur between molybdate species and chitosan-based sorbents, making the interpretation of sorption phenomena very complex.

REFERENCES

1. B. Volesky and Z. R. Holan, *Biotechnol. Prog.*, *11*, 235–250 (1995).
2. E. Guibal, C. Roulph, and P. Le Cloirec. *Water Res.*, *26*(8), 1139–1145 (1992).
3. S.-H. Lee and J. W. Yang, *Sep. Sci. Technol.*, *32*(8), 1371–1387 (1997).
4. C. L. Brierley, *Geomicrobiol. J.*, *8*, 201–223 (1990).
5. R. H. Crist, J. R. Martin, D. Carr, J. R. Watson, H. J. Clarke, and D. R. Crist, *Environ. Sci. Technol.*, *28*(11), 1859–1866 (1994).
6. B. Volesky and M. Tsezos, *Biotechnol. Bioeng.*, *24*, 385–401 (1982).
7. J. Chen, F. Tendeyong, and S. Yiacoumi, *Environ. Sci. Technol.*, *31*, 1433–1439 (1997).
8. J. Chen and S. Yiacoumi, *Sep. Sci. Technol.*, *32*(1–4), 51–69 (1997).
9. E. Guibal, M. Jansson-Charrier, I. Saucedo, and P. Le Cloirec, *Langmuir*, *11*(2), 591–598 (1995).
10. E. Guibal, C. Roulph, and P. Le Cloirec, *Environ. Sci. Technol.*, *29*(10), 2496–2503 (1995).
11. H. D. Ke, W. L. Anderson, R. M. Mocrief, and G. D. Rayson., *Ibid.*, *28*, 588 (1994).
12. C. F. Baes, Jr. and R. E. Mesmer, *Hydrolysis of Cations*, Wiley, New York, NY, 1986.
13. G. A. F. Roberts, *Chitin Chemistry*, Macmillan, London, 1992.
14. E. Guibal, C. Milot, and J. M. Tobin, *Ind. Eng. Chem. Res.*, *37*(4), 1454–1463 (1998).
15. E. Guibal, C. Milot, and J. Roussy, *Water Environ. Res.*, *71*(11), 10–17 (1999).
16. C. Milot, J. McBrien, S. Allen, and E. Guibal, *J. Appl. Polym. Sci.*, *68*, 571–580 (1998).
17. K. I. Draget, K. M. Vårum, E. Moen, H. Gynnild, and O. Smidsrød, *Biomaterials*, *13*(9), 635–638 (1992).
18. A. Baxter, M. Dillon, K. D. A. Taylor, and G. A. F. Roberts, *Int. J. Biol. Macromol.*, *14*, 166–169 (1992).
19. E. Piron, M. Accominotti and A. Domard, *Langmuir*, *13*, 1653–1658 (1997).
20. B. D. Gummow and G. A. F. Roberts, *Makromol. Chem.*, *186*, 1239–1244 (1985).
21. J. Rouquerol, D. Avnir, C. W. Fairbridge, D. H. Everett, J. H. Haynes, N. Pernicone, J. D. F. Ramsay, K. S. W. Sing, and K. K. Unger, *Pure Appl. Chem.*, *66*, 1739–1758 (1994).
22. D. L. Parkhurst, in *Chemical Modeling of Aqueous Systems II* (D. C. Melchior and R. L. Bassett, Eds.), American Chemical Society, Washington, DC, 1990.
23. A. Domard, *Int. J. Biol. Macromol.*, *9*, 98–104 (1987).
24. S. Boutamine, Z. Hank, M. Meklati, and O. Benali-Baitich, *J. Radioanal. Nucl. Chem. Articles*, *185*(2), 347–353 (1994).
25. P. Zhang, K. Inoue, and H. Tsuyama, *Energy Fuels*, *9*, 231–239 (1995).
26. Y. Zhao, A. I. Zouboulis, and K. A. Matis, *Sep. Sci. Technol.*, *31*(6), 769–785 (1996).
27. K. H. Von Tytko, G. Baethe, E. R. Hirschfeld, K. Mehmke, and D. Stellhorn, *Z. Anorg. Allg. Chem.*, *503*, 43–66 (1983).
28. M. T. Pope, "Polyoxoanions," in *Encyclopedia of Inorganic Chemistry*, *Vol. 1*, Wiley, New York, NY, 1994, pp. 3361–3370.

MARCEL DEKKER, INC.
270 Madison Avenue, New York, New York 10016

29. C. Papelis, K. F. Hayes, and J. O. Leckie, *HYDRAQL*: *A Program for the Computation of Chemical Equilibrium*, Technical Report 306, Environmental Engineering & Science, Department of Civil Engineering, Stanford University, Stanford, CA, September 1988.
30. R.-S. Juang and C.-Y. Ju, *Ind. Eng. Chem. Res.*, *36*, 5403–5409 (1997).
31. H. Yoshida, A. Okamoto, and T. Kataoka, *Chem. Eng. Sci.*, *48*, 2267–2272 (1993).
32. K. Inoue, Y. Baba, and K. Yoshizuka, *Bull. Chem. Soc. Jpn.*, *66*, 2915–2921 (1993).
33. K. Ohga, Y. Kurauchi, and H. Yanase. *Ibid*., *60*(1), 444–446 (1987).
34. P. Nekovár and D. Schrötterová, *Solv. Extr. Ion Exch.*, *17*(1), 163–175 (1999).
35. E. Guibal, C. Milot, A. Domard, and O. Eteradossi. *Int. J. Biol. Macromol.*, *24*(1), 49–59 (1999).

Received by editor June 1, 1999
Revision received October 1999

Request Permission or Order Reprints Instantly!